Meteorologische Zeitschrift, PrePub DOI 10.1127/metz/2017/0845


Climatology

# Seasonal Cycle in German Daily Precipitation Extremes

Madlen Fischer*, Henning W. Rust and Uwe Ulbrich

Institute of Meteorology, FU Berlin, Germany

(Manuscript received December 8, 2016; in revised form May 4, 2017; accepted July 13, 2017)

**Abstract**

The seasonal cycle of extreme precipitation in Germany is investigated by fitting statistical models to monthly maxima of daily precipitation sums for 2,865 rain gauges. The basis is a non-stationary generalized extreme value (GEV) distribution variation of location and scale parameters. The negative log-likelihood serves as the forecast error for a cross validation to select adequate orders of the harmonic functions for each station. For nearly all gauges considered, the seasonal model is more appropriate to estimate return levels on a monthly scale than a stationary GEV used for individual months. The 100-year return-levels show the influence of cyclones in the western, and convective events in the eastern part of Germany. In addition to resolving the seasonality, we use a simulation study to show that annual return levels can be estimated more precisely from a monthly-resolved seasonal model than from a stationary model based on annual maxima.

**Keywords:** Extreme value theory, Generalized Extreme Value (GEV) distribution, seasonal variations, extreme precipitation, rain gauge data, climate

## 1 Introduction

Extreme meteorological events such as heavy precipitation, strong winter storms or heat waves carry the potential for considerable damage and thus affect society (Intergovernmental Panel on Climate Change. Working Group II, 2014, and references therein). Threats due to precipitation can be either direct in the form of hail, freezing rain or flash floods, or indirect due to river flooding. Particularly for the latter, the seasonal timing of extreme precipitation is relevant; the risk of flooding is higher if the extreme precipitation coincides with already-high water levels due to, e.g., snow melt (Schindler et al., 2012a,b; Vormoor et al., 2015). Additionally, the seasonal cycle of extreme precipitation is important for the agricultural sector as it has an impact on crop yields: particularly during the early stages of plant reproduction, the crop is highly vulnerable to damage (Parry et al., 2005; Rosenzweig et al., 2001). Also for the replenishment of reservoirs in specific season, the monthly consideration of extreme precipitation might be interesting.

A widely accepted concept to describe the probability of occurrence, as well as the magnitude, of extreme events is extreme value statistics (EVS) (Beirlant et al., 2004; Coles, 2001; Embrechts et al., 1997). Countless applications of EVS have been applied in hydrology and climatology (e.g., Lerma et al., 2015; Arns et al., 2015; Brown and Katz, 1995; Coles and Tawn, 1996; Katz et al., 2002; Naveau et al., 2005; Cid et al., 2016; Friederichs, 2010), to name but a few. One way towards an assessment of extremes is the block maxima approach: the observed series is divided into blocks of equal length and one aims to model the probability distribution of maxima obtained from these blocks with the generalized extreme value distribution (GEV). For the choice of blocks for daily precipitation sums, popular strategies are: annual blocks (to avoid an explicit consideration of seasonality), monthly blocks followed by an individual treatment of each calendar month, or seasonal blocks (three-monthly block size). Here we propose a monthly block size, but instead of treating each calendar month separately, we explicitly account for seasonal variation in the model. This is realized by describing intra-annual variation of GEV parameters with a series of harmonic functions. This modelling approach is potentially superior to the treatment of individual months as it exploits the slow variations between individual months for parameter estimation; strength is thus "borrowed" from neighbouring calendar months. Furthermore, a description of the seasonality of extreme precipitation in terms of amplitude and phase can be achieved.

Although many applications do not directly require seasonally resolved return levels, e.g. the design of hydraulic structures is based on annual return levels, seasonality of extreme precipitation might enter indirectly via a possible coincidence with snow melt Bronstert (2003). However, exceedance probabilities for annual maxima (and thus annual return levels) can be obtained from exceedance probabilities of monthly maxima (monthly return levels) under the assumption of independence. Thus, the seasonal model is also a basis for estimating annual return levels. We demonstrate with a simulation study that the so derived annual return levels can be more precise than those derived with the annual block maxima approach.

The approach based on monthly block maxima and the description of their probability distribution with a

*Corresponding author: Madlen Fischer, Institute of Meteorology, FU Berlin, Carl-Heinrich-Becker-Weg 6–10, 12165 Berlin, e-mail: madlen.fischer@met.fu-berlin.de

non-stationary GEV was suggested in Rust et al. (2009) and Maraun et al. (2009) and exemplified with a UK case study. Here, we apply this concept for Germany and additionally carry out an explicit selection of orders in the harmonic series for individual stations based on cross validation. Apart from monthly resolved return levels, a further advantage of the seasonal modelling approach is a more precise estimation of annual return levels; this is demonstrated using a simulation study.

In summary, the aim of this study is a) to develop a gauge-based seasonally resolved climatology of extreme precipitation for Germany, b) to go technically beyond previous works by Rust et al. (2009) and Maraun et al. (2009) by carring out order selection and c) to show in a simulation study, that the return levels typically used in decision making are more accurate than for a annual approach without covariates.

We develop a seasonal extreme value model for daily precipitation sums for more than 2,800 rain gauges in Germany, presented in Section 2. The seasonal model is based on the GEV with monthly block maxima and is described in Section 3. There we also give the strategies for selecting between different seasonal models. We capture the seasonality using increasing orders of harmonic functions. Return levels, seasonality and seasons with the largest return levels for all stations are given in Section 4.1 and the procedure is illustrated for two synoptic stations in Section 4.2. We give annual return levels in Section 5 and discuss the results in Section 6.

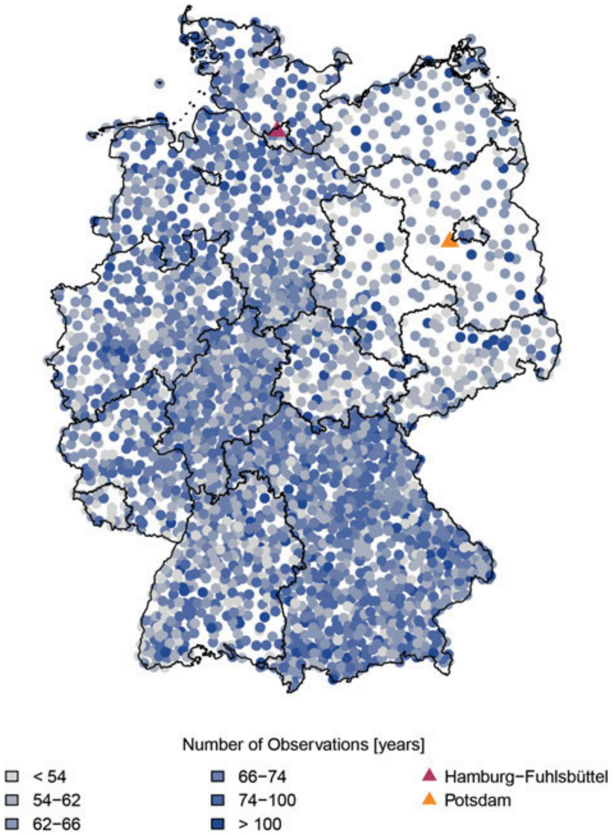


**Figure 1:** Number of observed years of 2,865 considered stations (observation period of at least 50 years). We discuss two stations in detail: Hamburg-Fuhlsbüttel (purple triangle) and Potsdam (orange triangle).

## 2 Data

A selection of gauges recording daily precipitation amounts have been obtained from the National Climate Data Center of the German Weather Service (Deutscher Wetterdienst, DWD). Daily precipitation amounts were measured with the Hellman rain gauge with a nominal accuracy of 0.1 mm for almost 5,600 stations. We consider a subset containing 2,865 time series covering an observation period of at least 50 years. It happens that some series contain days without observations (missing values) within their observation period. The number of available observations in years per station is depicted in Figure 1. The locations of the example stations Potsdam and Hamburg-Fuhlsbüttel are highlighted in orange and purple. The orography of Germany is given in Figure 2. For the present analysis, we consider the monthly maxima of daily precipitation amounts. Months with less than 27 days of measured values are discarded from the analysis.

## 3 Modelling extreme seasonal precipitation

Concepts from extreme value statistics (EVS) (Beirlant et al., 2004; Embrechts et al., 1997) can be used for an effective description of extreme precipitation. The two main routes of EVS are i) the peak-over-threshold approach, modelling excesses over a threshold with the generalized Pareto distribution, and ii) the block-maxima approach, using the generalized extreme value distribution (GEV) to describe the probability distribution of maxima drawn out of blocks of a certain size, e.g. monthly or annual maxima. An introduction to the topic is found in Coles (2001). Here, we follow the block maxima approach with a monthly block size and describe the resulting maxima with the GEV. The parameters of the GEV are allowed to smoothly vary throughout the year; the distribution of summer maxima has thus parameters different from the winter maxima. These smooth variations in parameters are modelled using series of harmonic functions. A cross validation experiment helps to determine a suitable order of these harmonic series for each station separately.

### 3.1 The block maxima approach

For a sequence of $n$ random variables $X_t$ ($t = 1, \ldots, n$), e.g. a series of daily precipitation, consider the maxima

$$M_n = \max\{X_1, \ldots, X_n\} \tag{3.1}$$

for a certain block length $n$, e.g. a month or a year. For independent and identically distributed random variables $X_t$ and a sufficient block size $n$ the Fisher-Tippett

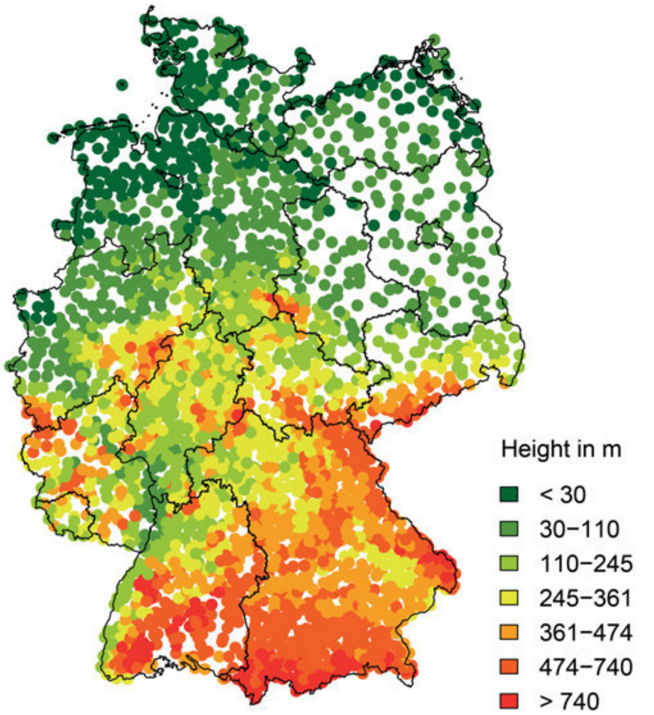


**Figure 2:** Altitude for all 2,865 considered stations.

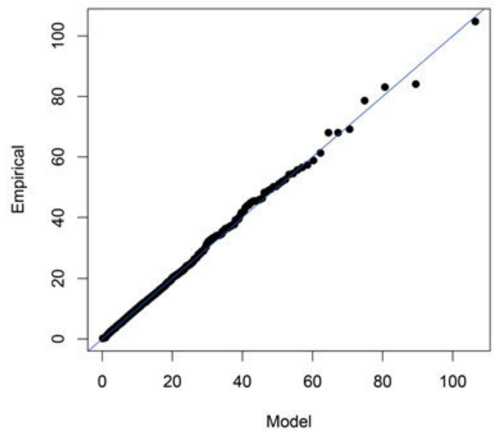


(a) Potsdam

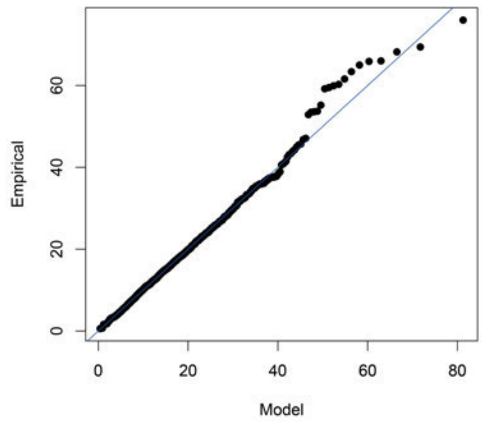


(b) Hamburg-Fuhlsbüttel

**Figure 3:** Q-Q-plot of the example stations Potsdam and Hamburg-Fuhlsbüttel.

theorem (Coles, 2001) states that either the Weibull, Gumbel or Fréchet distribution are suitable to describe the probability distribution function (PDF) of the maxima $M_n$. These three distributions can be summarised in the generalized extreme value distribution (GEV)

$$G(z;\mu,\sigma,\xi) = \exp\left\{-\left[1+\xi\left(\frac{z-\mu}{\sigma}\right)\right]^{-1/\xi}\right\} \quad (3.2)$$

with $\{z : 1+\xi(z-\mu)/\sigma > 0\}$. The location parameter $-\infty < \mu < \infty$ specifies the position of the probability density function (PDF), the scale parameter $\sigma > 0$ and shape parameter $-\infty < \xi < \infty$ determine the width and shape of the GEV, respectively. For a positive shape parameter $\xi > 0$, the PDF decay is slow (i.e. algebraic) towards large values; this is the case of the heavy tailed Frechet distribution. For a negative shape parameter $\xi < 0$, the GEV has a finite upper bound (Weibull distribution). The light tailed Gumbel distribution is obtained from the GEV in the limit $\xi \to 0$ and describes a fast (i.e. exponential) decay towards large values (Coles, 2001; Embrechts et al., 1997).

The Fisher-Tippett theorem thus suggests the GEV as a canonical model for block maxima, even for finite block size. Similar theorems not relying on the assumption of independent random variables are given in (Leadbetter et al., 1983, e.g.). The convergence rate of the block maxima towards the GEV depends on the nature of the underlying random variables and on their dependence (Embrechts et al., 1997); the impact on the convergence rate for a few classes of auto-correlated processes is exemplified in Rust (2009). Several studies (Rust et al., 2009; Maraun et al., 2009) suggest that a monthly block size is suitable for daily precipitation sums, at least in the mid-latitudes. Figure 3, showing the Q-Q-plots for the example stations, confirms the choice of a monthly block size for our data set.

## 3.2 Seasonally varying extreme value distribution

For many geoscientific applications it is hard to justify the assumption of a time-independent probability distribution for the block maxima $M_i$, particularly for a sub-annual sampling with seasonality resolved. In the present case, we expect precipitation maxima to vary along with the seasonal cycle. The block maxima approach based on the GEV allows for time-dependent parameters, and thus for describing the block maxima with a non-stationary GEV. To account for the periodic nature of the seasonal cycle, the time dependence of GEV parameters can be described with a series of harmonic functions with increasing order $m$, e.g., for the location parameter

$$\mu_t = \mu_0 + \sum_{m=1}^{M}(\mu_{m_{\sin}}\sin(m\omega c_t) + \mu_{m_{\cos}}\cos(m\omega c_t)), \quad (3.3)$$

with $t = 1, \dots, 12$ the months in the year, $c_t$ the centre of the $t$-th month given in days starting from January, 1st, $\omega = 2\pi/365.25$ the angular frequency of earth's rotation and $m = 1, \dots, M$ the order of harmonic functions used to model the location parameter (Rust et al., 2009; Maraun et al., 2009); sine and cosine are always used in pairs for a given order $m$.

Analogously, the seasonality of the scale parameter can be expressed as

$$\sigma_t = \sigma_0 + \sum_{n=1}^{N} (\sigma_{n_{\sin}} \sin(n\omega c_t) + \sigma_{n_{\cos}} \cos(n\omega c_t)). \quad (3.4)$$

with the order of harmonic function $n = 1, \dots, N$ for the scale parameter.

In principle, also the shape parameter could be described with a seasonal cycle. As this parameter is difficult to estimate and interferes with the estimation of the scale parameter (Ribereau et al., 2011), this is only meaningful if sufficient data is available. For all stations execpt one, we leave the shape parameter constant across the year, i.e. there is only one estimate of

$$\xi_t = \xi_0 \quad (3.5)$$

per rain gauge.

The parameters in the linear models for location, scale and shape are estimated by maximising the log-likelihood.

$$l(\boldsymbol{\theta}|z_i) = \sum_{i=1}^{I} \log g(z_i, |\boldsymbol{\theta}) \quad (3.6)$$

with $g(z_i, |\boldsymbol{\theta})$ being the probability density function of the GEV with the harmonic series $\mu_{m_{\sin}}, \mu_{m_{\cos}}$ and $\sigma_{n_{\sin}}, \sigma_{n_{\cos}}$ describing the seasonal dependence of location and scale and the constant shape $\xi_0$ being summarised in the parameter vector $\boldsymbol{\theta}$. The $z_i$ are the monthly maxima used for parameter estimation. Confidence intervals of the parameters are derived straight-forwardly based on the asymptotic properties of the Maximum-Likelihood-Estimator (Coles, 2001).

## 3.3 Return levels and return period

Extreme precipitation events are typically characterised by a pair of values specifying their magnitude (return level, $r_T$) and an associated expected time of their recurrence (return period, $T$). The return period $T$ is the average time an event of magnitude $r_T$ is expected to be exceeded once, e.g. a 100-year precipitation event specifies a magnitude ($r_{100}$) which is expected to be exceeded on average once every $T = 100$ years. In terms of probability distributions, the return level is the quantile of the maxima distribution (GEV) for a certain probability. A return level is thus obtained as

$$r_T = \begin{cases} \mu - \frac{\sigma}{\xi}[1 - y_T^{-\xi}] & \text{for} \quad \xi \neq 0 \\ \mu - \sigma \log y_T & \text{for} \quad \lim \xi \to 0 \end{cases}, \quad (3.7)$$

with $y_T = -\log(1/T)$. The return period $T = 1/(1-p)$ is related to the probability $p$ of a maximum not exceeding the return level $r_T$. Confidence intervals for return levels are derived from the GEV parameters using the *delta method* (Coles, 2001).

In engineering contexts, the 100-year or 1000-year return level is frequently the basis for designing structures, such as dams or bridges. As these return periods are typically larger then the length of the observation period, the model needs to be extrapolated beyond observations.

## 3.4 Model selection

It is *a priori* not evident which order of the harmonic series in $\mu$ and $\sigma$ is adequate to describe the seasonal variability. We determine orders using cross validation (CV). The main idea of CV is to split the full data set $S$ into $K$ subsets $S_k, k = 1, \dots, K$ and use $K - 1$ subsets to estimate model parameters and the remaining subset $S_{\bar{k}}$ to obtain a prediction error for the data points not used for parameter estimation. Here, subset always contain full years. Subsequently, subsets are exchanged and a prediction error is obtained for another subset. This procedure is repeated until a prediction error has been obtained for all $K$ subsets $S_k$. Combining the prediction error for all subsets yields the cross validation error (CVE). The prediction error is quantified using the negative log-likelihood

$$D_k(z_i|i \in S_k) = -l(\theta_{\bar{k}}|z_i, i \in S_k) \quad (3.8)$$

with $l(\theta_{\bar{k}}|z_i, i \in S_k)$ denoting the likelihood evaluated for maxima in $S_{\bar{k}}$ but with parameters obtained from $S_k$.

The CVE for one station is obtained by summing over all subsets

$$CVE = \sum_{k}^{K} D_k(z_i|i \in S_k). \quad (3.9)$$

Here, we use $K = 10$ and thus randomly split each of the records into 10 parts, each part contains full years of observations. For the location and scale parameters, we consider harmonic functions up to order five including a zero order (constant parameter throughout the year). Thus, 36 variants of different combinations of harmonic orders are tested for each station. The most flexible model contains 23 coefficients (11 for each location and scale, and 1 for shape).

In addition, we set up a reference model: the maxima of each month of the year are described by a stationary GEV; a strategy frequently used in practice. This leads to 12 different sets of parameters - location, scale and shape for each month, and thus 36 parameters in total. This formulation allows for a seasonally varying shape parameter.

For about 31 % of all stations it is impossible to obtain a CVE for the reference model, since the validation data set includes values outside the support of the

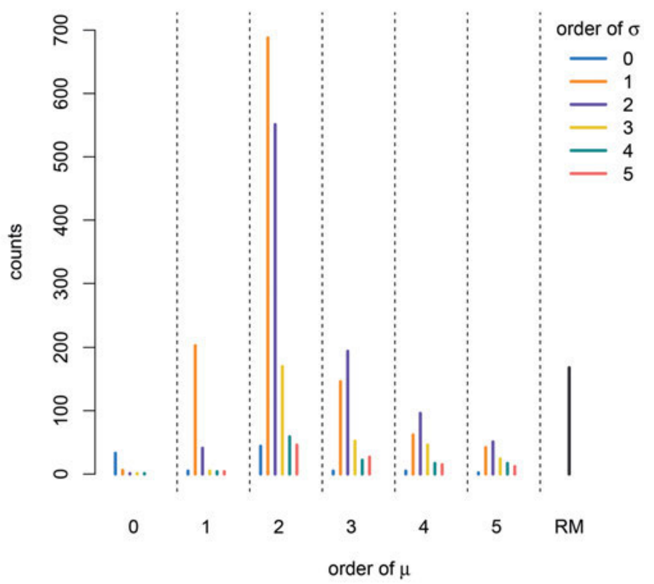


**Figure 4:** Number of stations for the best seasonal models. The order of harmonic functions in $\mu$ is depicted on the x-axis and order in $\sigma$ is coloured. The grey bar depicts the number of stations preferring the reference model (RM).

GEV found for the training data set, which is typically the case for $\xi < 0$, resulting in a GEV with an upper bound. This results in an occurrence probability equal to zero and an undefined log-likelihood. Thus, this model is highly unsuitable to describe the data sets of these stations. The CRPS as a scoring rule based on the GEV (closed form given by FRIEDERICHS and THORARINSDOTTIR, 2012) would not exhibit the problem of non-calculability. Here, however, we want to highlight this case as it might lead to severe consequences.

For 168 stations (5.9 % of all time series) the considered seasonal models do not provide a smaller CVE than the reference model. These stations are mainly characterised by very high seasonal variations which can not be represented by a constant shape parameter. For these 168 stations the reference model is considered to estimate the return levels. Figure 4, showing the frequency of the best seasonal models, illustrates that the majority of stations (~ 52 %) prefer a first or second order in $\mu$ and $\sigma$.

# 4 Monthly return levels

## 4.1 Results for all stations

### 4.1.1 100-year return level

This section covers the seasonal 100-year return levels for all 2,865 stations. Figure 5 depicts the return levels in mm/day for each month. Orographic effects lead to larger rainfall amounts for higher altitudes and thus also to more intense extreme precipitation events. This is confirmed by Figure 6, which shows the return levels

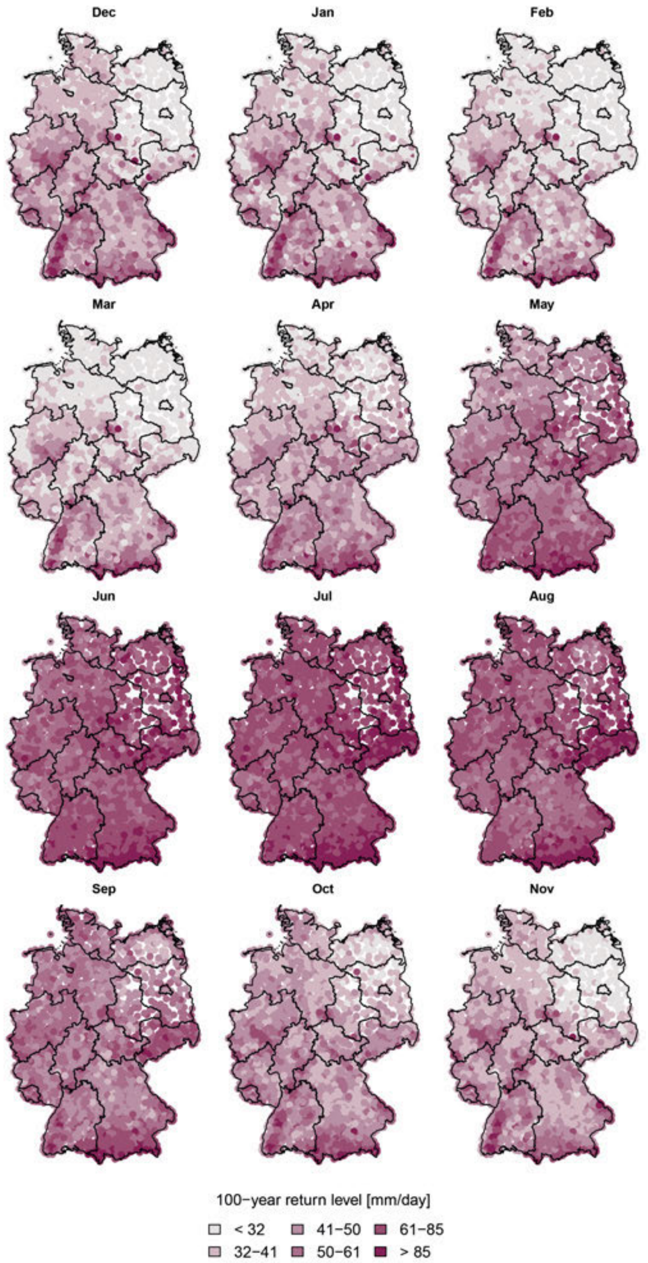


**Figure 5:** 100-year return levels in mm/day conditioned on the month of their occurrence for 2,865 stations (dots). The panel show the month December to November left to right and top to bottom.

with respect to the altitude for each calendar month. Some stations with higher elevation and lower return levels indicate that other aspects might be relevant for extreme precipitation as well, e.g. the direction of the incoming flow with respect to the orography.

In addition to this, Figure 5 shows that in January the spatial differences are very pronounced, with the highest return levels at stations of higher elevation and the lowest in the north-east of Germany. The values increase from south to north with variation in time and reach a maximum at most of the stations in summer. But in some regions, for example the Black Forest or the Harz, the return levels slightly decrease such that the spatial pattern in summer is more uniform. Until December the return

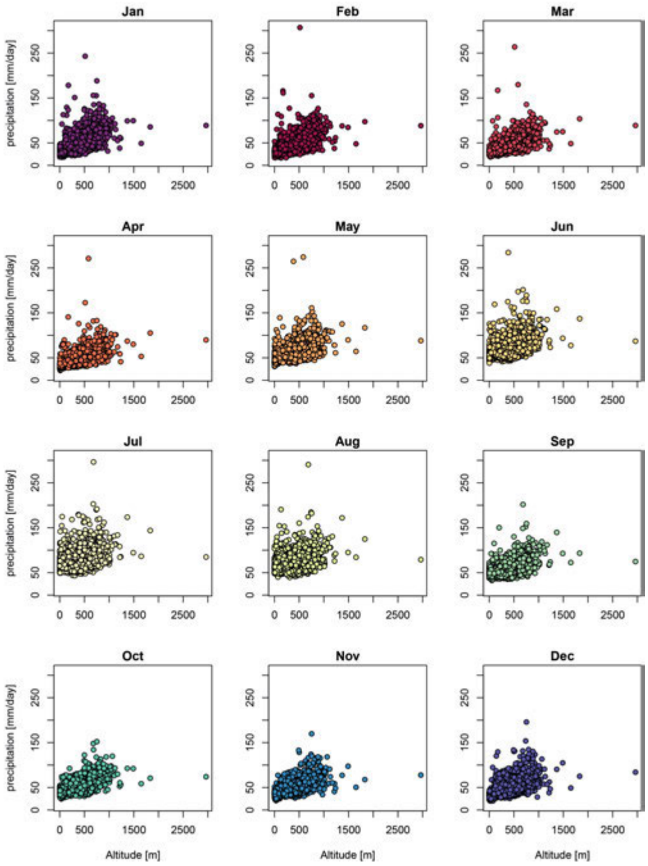


**Figure 6:** 100-year return levels in mm/day with respect to the altitude of the station for the individual months.

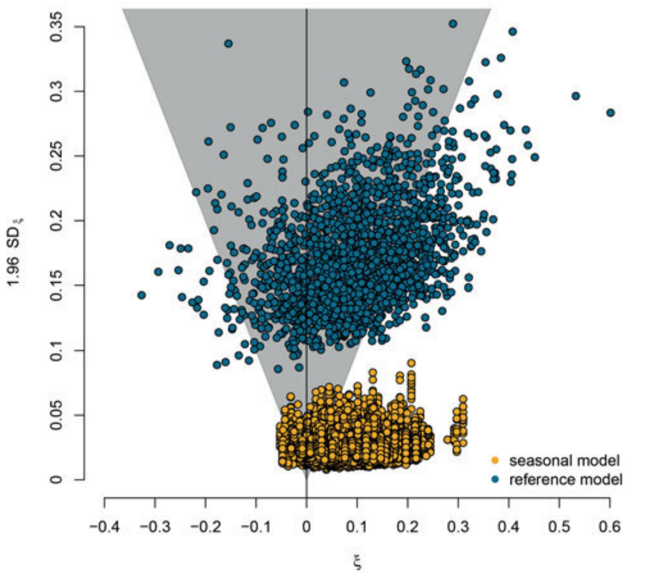


**Figure 7:** Scatterplots of $1.96SD_\xi$ against $\xi$ for the 168 stations preferring the reference model (blue) and the remaining stations preferring a seasonal model (yellow); estimates inside the grey-shading are not significant on a 95 % level based on asymptotic normality of the estimator.

levels decreased from north to south and show nearly the same pattern as in January.

As the shape parameter has a strong influence on large return levels, its value and uncertainty is of key interest for practical applications. Figure 7 shows $1.96\mathrm{SD}_\xi$ against the estimate $\xi$; in blue the 168 stations preferring the reference model and in yellow the remaining stations with a seasonal model. Estimates inside the grey area are not significantly different from zero based on asymptotic normality of the estimator and a 95 % level of significance. Estimates from the seasonal model (yellow) show a considerably smaller standard deviation and thus a lot more estimates can be considered to be different from zero.

### 4.1.2 Amplitude

In addition to the return levels for each month, the amplitude of the seasonal variations is interesting to describe extreme precipitation. For a given return period we seek to characterise the amplitude using

$$A_{\%} = \frac{r_{T_{\max}} - r_{T_{\min}}}{r_{T_{\max}} + r_{T_{\min}}} \cdot 100\,\% \tag{4.1}$$

with $r_{T_{\max}}$ denoting the maximum and $r_{T_{\min}}$ the minimum return level over all months in the year.

In Figure 8 the amplitudes are depicted for all stations, with small/large values indicating weak/strong seasonality. Assuming that the climate is more continental in the east (convective precipitation events dominate in summer) and more maritime in the west of Germany (frontal precipitation dominating) the main results can be summarised as:

- Very pronounced intra-annual variations at stations in the east and the valleys: higher influence of heavy convective precipitation in summer
- Less seasonal variations at stations further west (higher maritime influence) due to a more dominant all-year stratiform precipitation
- Weakest seasonality at stations with high elevation: lift of air masses and accumulation effects lead to all-year unchanged extreme precipitation

### 4.1.3 Phase

Finally, the month of the maximum 100-year return level (phase of seasonal variations) is depicted in Figure 9. In particular for the agricultural and tourist sector, or for filling reservoirs, the months of the most intense extremes are of special interest. In the eastern part of Germany the highest precipitation is typically found in June/July. At many stations further west but still in the lowlands, the highest return levels occur from August to October. This could be an indicator of the influence of increased cyclone activity in autumn and thus a larger contribution from stratiform precipitation. Some high altitudes, i.e. the Harz, the Black Forest and the Bavarian Forest, are characterised by a precipitation maximum in the winter months. In addition to the station's elevation, the relation between orographic structure and main wind

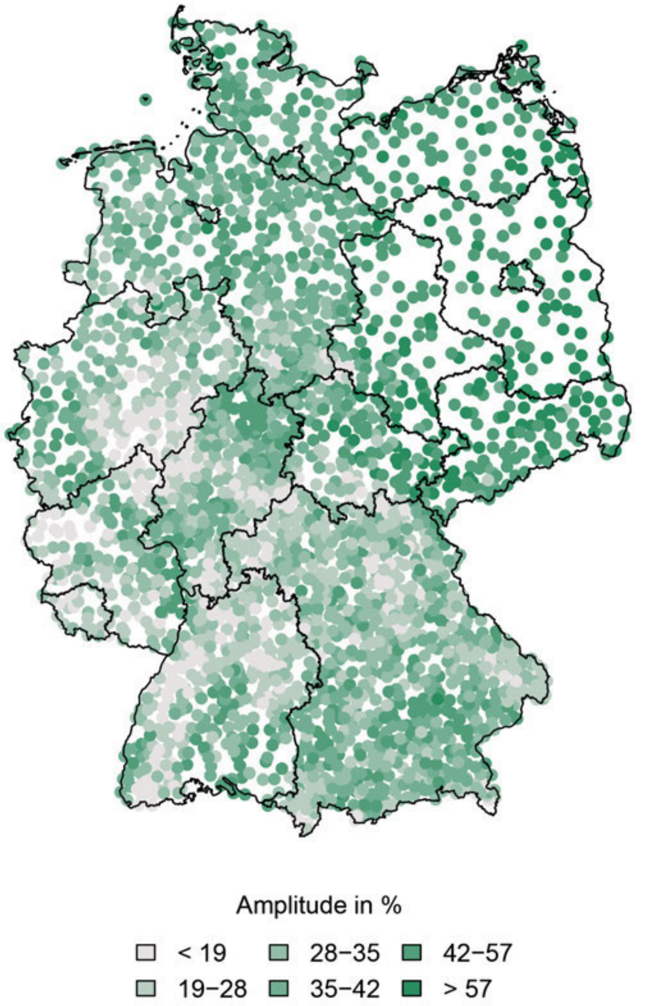


**Figure 8:** Percentage amplitude of the intra-annual variations of the 100-year return levels for 2,865 stations. Large/small values indicate a strong/weak seasonality.

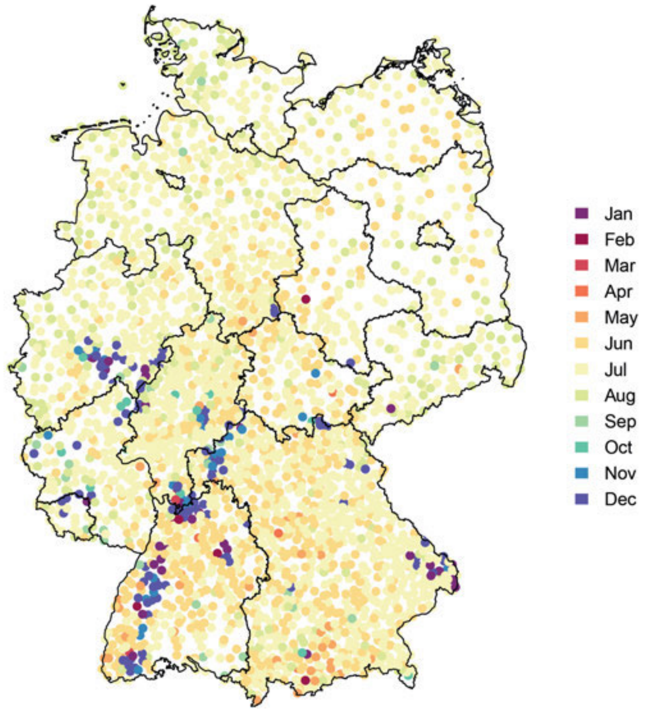


**Figure 9:** Month of occurrence of the maximum 100-year return level in the year for 2,865 stations indicating the time of the year when extreme precipitation events are strongest.

direction is an important factor. If a mountain chain lies perpendicular to the main wind direction (west, strongest storminess in winter) the lifting effects and the connected convection are maximised and thus lead to high precipitation amounts, particularly in winter.

## 4.2 Results for example stations

The first example station shows a case where the seasonal approach provides quite good results. The data set of the station Potsdam (orange triangle in Figure 1) covers the period from 01.01.1893 to 31.05.2016. The monthly maxima of the observed daily precipitation amounts are shown in Figure 10 as Box-Whisker-Plots (grey). The black line within the box denotes the median, the upper and lower bound of the box the 0.75 and 0.25 percentile. The whiskers describe the maximum and minimum value if they are closer to the median than the 1.5 inter-quartile range. Data points outside the whiskers are plotted as open circles. Strong evidence for significant differences of the medians exists if the notches of two boxes do not overlap. In addition to this, the 0.99 percentile of the observation is marked with a horizontal black line for each month. Return levels from the seasonal model with corresponding 95 % confidence interval are shown as solid lines and shadows coloured in yellow to blue for the non-exceeding probabilities $p = 0.25, 0.5, 0.75, 0.99$. At the station Potsdam, the seasonal model containing a second order in location, first order in scale and no seasonal variations in shape, which is labeled 2.1.0, is preferred. The 0.25-, 0.5- and 0.75 quantiles reflect the lower and upper quartile and the median of the observed precipitation amounts very well. Due to the large amount of available data points the confidence intervals are small. A suitable approach to investigate the quality of the 100-year return level is to count the precipitation events above the 0.99 quantile line. Because of an observation period of nearly 123 years in Potsdam, 1.23 exceedings per month, or rather 15 exceedings per year are expected. As shown in Figure 10, 16 daily precipitation events exceed the 0.99 quantile. Including the confidence intervals the model can represent the observed maxima very well.

One of the 168 stations favouring the reference model is presented to exemplify the potential improvement of the applied seasonal approach. The data record of the station Hamburg-Fuhlsbüttel (purple triangle in Figure 1) is characterised by a long observation period from 01.01.1891 to 31.05.2016. The monthly maxima and the seasonal return levels are shown in Figure 11. In addition to the result of the favoured reference model in Figure 11a) the best seasonal model 3.3.0 (third order in $\mu$ and $\sigma$ and a constant $\xi$) is shown in b) as well.

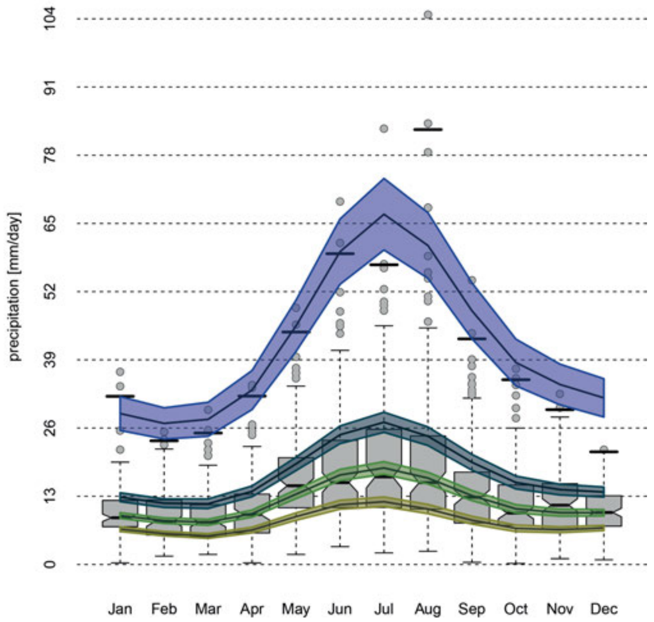


**Figure 10:** Box-Whisker-Plots (light grey) of monthly maxima of observed daily precipitation amounts for the example station Potsdam (01.01.1893–31.05.2016) and the return levels (black curves) obtained by the seasonal model 2.1.0 (second order in $\mu$, first order in $\sigma$ and constant $\xi$) for $p = 0.25, 0.5, 0.75, 0.99$ (from the bottom up) with their 95 %-confidence intervals (coloured area). The black horizontal lines label the 0.99 percentile determined from the observed data.

Since Hamburg-Fuhlsbüttel has a quite long observation record, it is possible here to also vary the shape parameter in time according to Eq. 3.3 and 3.4. The thus obtained 2.2.1 model (second order in $\mu$ and $\sigma$ and first order in $\xi$) provides a smaller CVE than the reference model (Figure 11c)). Adding the variation in $\xi$ to the seasonal model (from Figure 11b) to Figure 11c)) do not only improves the CVE but also reduces the amount of necessary coefficients from 15 to 13. Additionally, it can be noted that the reference model can represent the observations very well, especially for lower return levels. The 100-year return levels (blue curve), which are of greater benefit in the engineering context, are however highly uncertain. Since the seasonal models combine data from all months, this uncertainty is clearly reduced. Adding seasonal variations in the shape parameter allow uncertainties to slightly rise again, in particular for higher return levels. Additionally, the model is able to capture the peak of rare extreme events in August. For the long time series of Hamburg-Fuhlsbüttel, it is possible and necessary to allow the seasonal variations in the shape parameter as well. This option is subject to further investigation. For shorter series a spatial model for the GEV which considers all stations simultaneously might allow also for a seasonally varying shape parameter. A variable shape parameter might as well be useful in terms of a meteorological interpretation, since the character of extreme precipitation varies in general from stratiform precipitation in winter and convective events in summer.

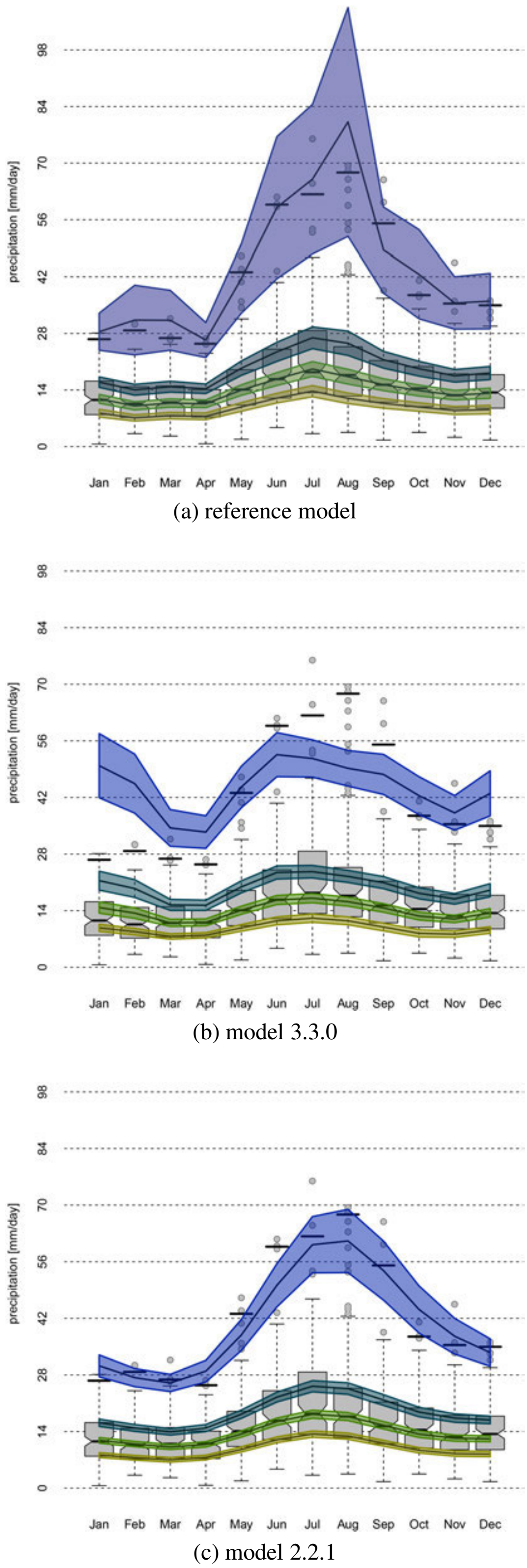


**Figure 11:** Box-Whisker-Plots (light grey) of monthly maxima of observed daily precipitation amounts for the example station Hamburg-Fuhlsbüttel (01.01.1891–31.05.2016) and the return levels (black curves) calculated with a) the stationary approach, b) the seasonal model 3.3.0 (third order in $\mu$ and $\sigma$ and constant $\xi$) and c) the seasonal model 2.2.1 (second order in $\mu$ and $\sigma$ and first order in $\xi$) for $p = 0.25, 0.5, 0.75, 0.99$ (from the bottom up) with their 95 %-confidence intervals (coloured area). The black horizontal lines label the 0.99 percentile determined from the observed data.

## 5 Annual return levels

For many applications in the field of hydraulic design and risk assessment, the annual return levels are more relevant than the monthly resolved levels. Commonly, the GEV (Eq. 3.2) is used to describe annual maxima and to estimate annual return levels. However, annual return levels can also be obtained from the seasonal model. The $T$-year annual return level $r_T$ can be derived from the non-stationary model by numerically solving the following equation (Maraun et al., 2009):

$$\prod_{i=1}^{12} G_i(r_T) = 1 - \frac{1}{T} \tag{5.1}$$

with $G_i(r_T)$ being the probability of the occurrence of a value smaller than $r_T$ in the month $i$. This approach assumes independent maxima of the different months. Figure 12 shows the annual 100-year return levels determined from the best seasonal model for each station. The return levels are characterised by higher values in the east of Germany and in mountainous regions with more than 128 mm/day. In the Alps the return levels even reach values up to 298 mm/day. As already mentioned in Section 4.1.1 for monthly return levels, there are further important aspects, e.g. the direction of the incoming flow, which might explain the pattern of the annual return levels as well.

### 5.1 Simulation study

To illustrate the improvement of obtaining annual return levels derived from the seasonal model compared to directly modelling annual maxima with the GEV, we carry out the following simulation study: We generate series of monthly maxima using GEV-distributed random variables with a typical seasonal component in location and scale (model 1.2.0: first order in $\mu$, second order in $\sigma$, constant $\xi$). The values for the different parameters are shown in Table 1.

On the basis of these monthly maxima series we apply two strategies for deriving annual return levels: 1) obtain annual maxima and estimate parameters for a stationary GEV (annual approach), and 2) model the annual maxima with a seasonal GEV model (seasonal approach). We generate series of different length (12 years to 600 years), 10,000 iterations each. Since we assume that the model selection determine the right order of harmonic function, we also use the 1.2.0 model to obtain annual return levels for approach 2). The results of both strategies are compared with the model used for generation considering the Mean Squared Error (MSE) for the return levels over all iterations $N$:

$$\text{MSE} = \frac{1}{N}\sum_{n=1}^{N}(r_T - r_{T_{\text{ref}}})^2 \tag{5.2}$$

with $r_T$ being the return levels derived from one of the modelling methods for annual maxima and $r_{T_{\text{ref}}}$ being

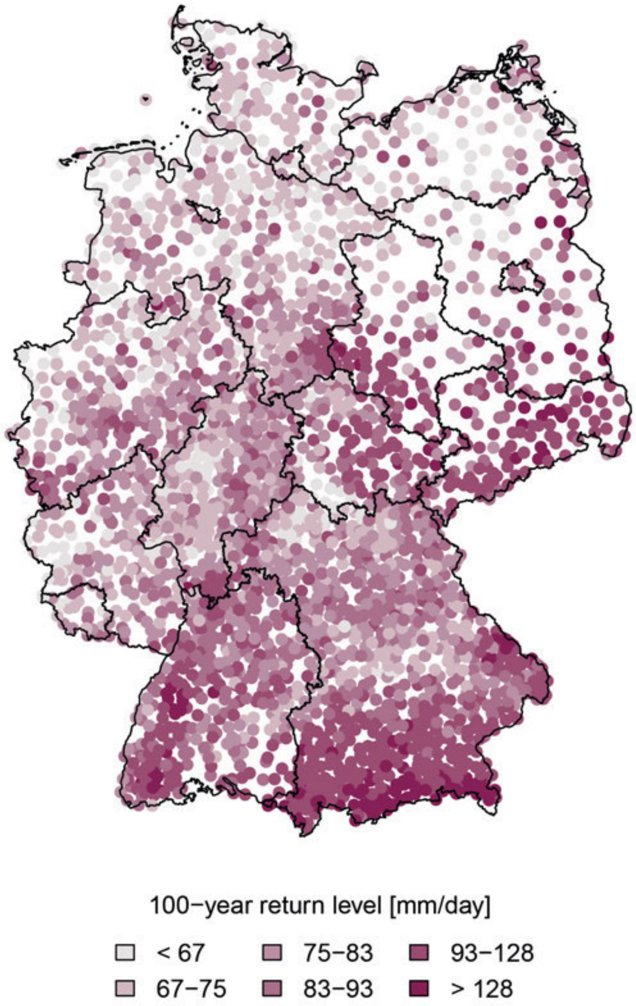


**Figure 12:** Annual 100-year return levels in mm/day derived from the best seasonal model for each of the 2,865 stations.

**Table 1:** Parameters of the model used for generation of GEV-distributed random variables with a first order in location, second order in scale and constant shape.

| $\mu_0$ | $\mu_{1_{\sin}}$ | $\mu_{1_{\cos}}$ | $\sigma_0$ | $\sigma_{1_{\sin}}$ | $\sigma_{1_{\cos}}$ | $\sigma_{2_{\sin}}$ | $\sigma_{2_{\cos}}$ | $\xi_0$ |
|---|---|---|---|---|---|---|---|---|
| 10.2 | −0.6 | −3.1 | 5.5 | −0.5 | −2 | 0.4 | 0.05 | 0.1 |

the annual return level derived from the model of generation (Tab. 1) using Eq. 5.1.

Figure 13 shows the MSE and the bias ($r_T - r_{T_{\text{ref}}}$) for the annual return levels obtained using 1) (dashed lines) and 2) (solid lines) for 50-year (green), 100-year (blue) and 1,000-year (red) return levels. The variance of the return levels does not differ visually from the results of the MSE (not shown). Both, MSE and bias of annual return levels derived from the seasonal model are significantly smaller than for the standard approach based on annual maxima, particularly for the important cases with short record lengths and long return periods. For a typical observation length of 60 years in Germany and the often used 100-year return level, the MSE of method 2) is reduced by nearly 31 % with respect to method 1).

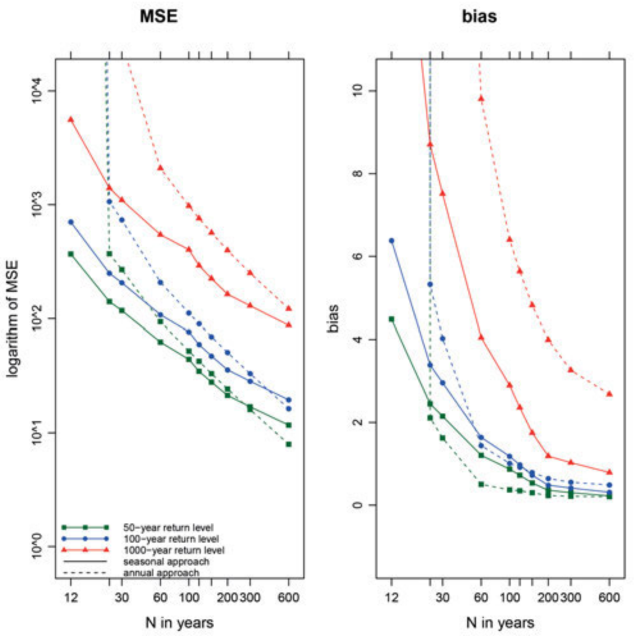


**Figure 13:** MSE and bias of annual return levels calculated from a generated data set using a annual approach (dashed lines) and a seasonal approach (solid lines) for different return periods (50-year: green, 100-year: blue, 1000-year: red) and for different series lengths (x-axis). The variances of the return levels do not differ visually from the MSE (not shown).

Assuming that the model selection is not able to find the right order of harmonic functions, we also analysed different seasonal models to obtain the annual maxima (not shown). It turns out that annual return levels can be derived more accurately with strategy 2) as long as the seasonal model used in estimating parameters is not less complex than the seasonality present in the data.

## 6 Summary and discussion

We describe monthly maxima of daily precipitation amounts of 2,865 stations in Germany with a seasonal Generalized Extreme Value (GEV) distribution to explicitly resolve seasonality. This is realized using harmonic functions of different orders for the location and scale parameter of the GEV, the shape parameter is held constant in time. In contrast to previous publications (e.g., Rust et al., 2009; Maraun et al., 2009), order selection for the harmonic series for each station is separately carried out using cross validation.

Only 168 of the 2,865 stations considered suggest that our setup of seasonal models (orders from 0 to 5 for location and scale parameter) is not sufficient to characterise a more complex seasonal variation of very extreme events (e.g. 100-year return level). For these stations we apply a modelling approach with a GEV for each month separately. However, for one long series, we explored the possibility of a seasonally varying shape as well. The result suggests that a seasonal variation in the shape parameter might be beneficial if there is sufficient data to estimate the variation. As data for extremes is frequently sparse at individual stations, a spatial approach might help to estimate seasonality in the shape parameter. Such a strategy is currently under investigation by the authors including the unknown functional relationship between the GEV parameters and the spatial covariates using Legendre Polynomials to ensure independence of the terms, a method suggest by Rust et al. (2013) and Ambrosino et al. (2011). Other spatial modelling approaches are, for example, the Regional Frequency Analysis (Hosking and Wallis, 2005; Soltyk et al., 2014) where regions of similar statistical characteristics are combined and common probabilities for extremes are obtained, or Bayesian Hierarchical Models (i.e. Cooley et al., 2007; i.e. Davison et al., 2012) where the spatial variations are taken care of by a large-scale contribution described with linear regression and local variations captured by a spatial stochastic process. A non-parametric way of modelling spatial variations can be realized with generalized additive models (GAM) (i.e. Stauffer et al., 2016; Simon et al., 2017). We expect that a spatial approach does not only provide information at ungauged sites but also improves accuracy of return-level estimates, particularly for long return-periods.

For all other stations the seasonal approach described provides a very good representation of the data sets and reduces the uncertainty of the return levels. In addition to resolving seasonality, we compare two ways of estimating annual return levels: 1) the classical approach based on annual maxima described with the GEV and 2) the approach proposed here based on monthly maxima and a seasonal GEV. To this end, we carry out a simulation study, which demonstrates the improvement in estimating annual return levels derived from the seasonal model with respect to the return levels based on annual maxima. MSE and bias of the two approaches are compared and it turns out that the annual return levels derived from the seasonal model and monthly maxima are more accurate, particularly for short series and long return periods. This is plausible as the monthly scale carries more information which facilitates parameter estimation, particularly together with the assumption of smoothly varying parameters throughout the year and a parsimonious parametric model describing this variation. It is thus consequent, that annual return levels can be estimated more accurately and more robustly with the approach presented here.

## Acknowledgements

We are greatful to two anonymous referees as well as to the editor Petra Friederichs for valuable comments which led to an improvement of the manuscript! This study has been funded by the Deutsche Forschungsgemeinschaft (DFG), partially through the research training school "NatRiskChange" GRK 2043/1 and partially through grant CRC 1114 "Scaling Cascades in Complex Systems", Project A01: Coupling a multiscale stochastic precipitation model to large scale atmospheric flow dynamics. The authors additionally thank the National Climate Data Center of the German Weather Service (DWD) for providing and maintaining the precipitation data sets via the online portal WebWerdis (https://werdis.dwd.de). The analysis was carried out with software written in R (R Core Team, 2014), based on the ismev package (Heffernan and Stephenson, 2014) and evd package (Stephenson, 2002).

## References

Ambrosino, C., R.E. Chandler, M.C. Todd, 2011: Southern african monthly rainfall variability: An analysis based on generalized linear models. – J. Climate **24**, 4600–4617.

Arns, A., T. Wahl, I.D. Haigh, J. Jensen, 2015: Determining return water levels at ungauged coastal sites: a case study for northern Germany. – Ocean Dyn. **65**, 539–554.

Beirlant, J., Y. Goegebeur, H. Segers, J. Teugels, 2004: Statistics of Extremes: Theory and Applications. Series in Probability and Statistics. – Wiley.

Bronstert, A., 2003: Floods and climate change: interactions and impacts. – Risk Analysis **23**, 545–557.

Brown, B.G., R.W. Katz, 1995: Regional analysis of temperature extremes: spatial analog for climate change? – J. Climate **8**, 108–119.

Cid, A., M. Menéndez, S. Castanedo, A.J. Abascal, F.J. Méndez, R. Medina, 2016: Long-term changes in the frequency, intensity and duration of extreme storm surge events in southern Europe. – Climate Dyn. **46**, 1503–1516.

Coles, S.G., 2001: An Introduction to Statistical Modelling of Extreme Values. – Springer, London.

Coles, S.G., J.A. Tawn, 1996: A Bayesian analysis of extreme rainfall data. – Appl. Stat. **45**, 463–478.

Cooley, D., D. Nychka, P. Naveau, 2007: Bayesian spatial modeling of extreme precipitation return levels. – J. Amer. Stat. Ass. **102**, 824–840.

Davison, A.C., S. Padoan, M. Ribatet, 2012: Statistical modeling of spatial extremes. – Statistical Sci. **27**, 161–186.

Embrechts, P., C. Klüppelberger, T. Mikosch, 1997: Modelling Extremal Events for Insurance and Fincance. – Springer, Berlin.

Friederichs, P., 2010: Statistical downscaling of extreme precipitation events using extreme value theory. – Extremes **13**, 109–132.

Friederichs, P., T.L. Thorarinsdottir, 2012: Forecast verification for extreme value distributions with an application to probabilistic peak wind prediction. – Environmetrics **23**, 579–594.

Heffernan, J.E., A.G. Stephenson, 2014: ismev: An Introduction to Statistical Modeling of Extreme Values. – R package version 1.40.

Hosking, J.R.M., J.R. Wallis, 2005: Regional frequency analysis: an approach based on L-moments. – Cambridge University Press.

Intergovernmental Panel on Climate Change. Working Group II, 2014: Climate Change 2014: Impacts, Adaptation, and Vulnerability. Part A: Global and Sectoral Aspects. Contribution of Working Group II to the Fifth Assessment Report of the Intergovernmental Panel on Climate Change. Field, C.B., V.R. Barros, D.J. Dokken, K.J. Mach, M.D. Mastrandrea, T.E. Bilir, M. Chatterjee, K.L. Ebi, Y.O. Estrada, R.C. Genova, B. Girma, E.S. Kissel, A.N. Levy, S. MacCracken, P.R. Mastrandrea, L.L.White (eds.). – Cambridge University Press, Cambridge, United Kingdom and New York, NY, USA, 1132 pp.

Katz, R.W., M.B. Parlange, P. Naveau, 2002: Statistics of extremes in hydrology. – Adv. Water Resour. **25**, 1287–1304.

Leadbetter, M.R., G. Lindgren, H. Rootzén, 1983: Extremes and related properties of random sequences and processes. Springer Series in Statistics. – Springer, New York.

Lerma, A.N., T. Bulteau, S. Lecacheux, D. Idier, 2015: Spatial variability of extreme wave height along the atlantic and channel french coast. – Ocean Eng. **97**, 175–185.

Maraun, D., H.W. Rust, T.J. Osborn, 2009: The annual cycle of heavy precipitation across the UK: a model based on extreme value statistics. – J. Climatol. **29**, 1731–1744.

Naveau, P., M. Nogaj, C. Ammann, P. Yiou, D. Cooley, V. Jomelli, 2005: Statistical methods for the analysis of climate extremes. – C.R. Geosci. **377**, 1013–1022.

Parry, M., C. Rosenzweig, M. Livermore, 2005: Climate change, global food supply and risk of hunger. – Philosophical Transactions of the Royal Society of London B: Biological Sciences **360**, 2125–2138.

R Core Team, 2014: R: A Language and Environment for Statistical Computing. – R Foundation for Statistical Computing, Vienna, Austria.

Ribereau, P., P. Naveau, A. Guillou, 2011: A note of caution when interpreting parameters of the distribution of excesses. – Adv. Water Resour. **34**, 1215–1221, DOI: 10.1016/j.advwatres.2011.05.003.

Rosenzweig, C., A. Iglesias, X. Yang, P.R. Epstein, E. Chivian, 2001: Climate change and extreme weather events; implications for food production, plant diseases, and pests. – Global change & human health **2**, 90–104.

Rust, H.W., 2009: The effect of long-range dependence on modelling extremes with the generalised extreme value distribution. – Europ. Phys. J. Special Topics **174**, 91–97.

Rust, H.W., D. Maraun, T.J. Osborn, 2009: Modelling seasonality in extreme rainfall: a UK case study. – Europ. Phys. J. Special Topics **174**, 99–111.

Rust, H.W., M. Vrac, B. Sultan, M. Lengaigne, 2013: Mapping weather-type influence on Senegal precipitation based on a spatial–temporal statistical model. – J. Climate **26**, 8189–8209.

Schindler, A., D. Maraun, A. Toreti, J. Luterbacher, 2012a: Changes in the annual cycle of heavy precipitation across the british isles within the 21st century. – Env. Res. Lett. **7**, 044029.

Schindler, A., D. Maraun, J. Luterbacher, 2012b: Validation of the present day annual cycle in heavy precipitation over the british islands simulated by 14 RCMs. – J. Geophys. Res. Atmos. **117**, published online. DOI: 10.1029/2012JD017828.

Simon, T., N. Umlauf, A. Zeileis, G.J. Mayr, W. Schulz, G. Diendorfer, 2017: Spatio-temporal modelling of lightning climatologies for complex terrain. – Natural Hazards Earth Sys. Sci. **17**, 305–314.

Soltyk, S., M. Leonard, A. Phatak, E. Lehmann, others, 2014: Statistical modelling of rainfall intensity-frequency-duration curves using regional frequency analysis and bayesian hierarchical modelling. – In: Hydrol. Water Resour. Symp. 2014, 302, Engineers Australia.

Stauffer, R., G.J. Mayr, J.W. Messner, N. Umlauf, A. Zeileis, 2016: Spatio-temporal precipitation climatology over complex terrain using a censored additive regression model. – Int. J. Climatol. **37**, 3264–3275. DOI: 10.1002/joc.4913.

Stephenson, A.G., 2002: evd: Extreme value distributions. – R News **2**, 31–32.

Vormoor, K., D. Lawrence, M. Heistermann, A. Bronstert, 2015: Climate change impacts on the seasonality and generation processes of floods–projections and uncertainties for catchments with mixed snowmelt/rainfall regimes. – Hydrol. Earth Sys. Sci. **19**, 913–931.